GEOPHYSICAL RESEARCH LETTERS, VOL. 35, L17S04, doi:10.1029/2007GL033033, 2008

THEMIS observations of modified Hall fields in asymmetric magnetic field reconnection

F. S. Mozer,[1] V. Angelopoulos,[1] J. Bonnell,[1] K. H. Glassmeier,[2] and J. P. McFadden[1]

Received 18 December 2007; revised 18 February 2008; accepted 5 March 2008; published 18 April 2008.

[1] Field and plasma measurements from three THEMIS spacecraft are compared during a back-and-forth crossing of an asymmetric, reconnecting, sub-solar magnetopause to explain the apparent absence of the quadrupolar magnetic field and part of the bipolar electric field that are found during symmetric magnetic field reconnection. The differences in the reconnection magnetic fields in the asymptotic regions (a factor of three) and the plasma densities (a factor of 30) combine to make the Hall MHD term and the resulting Hall electric field in the Generalized Ohm's law significant only on the magnetospheric side of the magnetopause. Qualitative analysis indicates that the single particle and fluid trajectories in such fields are different from those in the case of symmetric boundary conditions. **Citation:** Mozer, F. S., V. Angelopoulos, J. Bonnell, K. H. Glassmeier, and J. P. McFadden (2008), THEMIS observations of modified Hall fields in asymmetric magnetic field reconnection, *Geophys. Res. Lett.*, *35*, L17S04, doi:10.1029/2007GL033033.

1. Introduction

[2] The Generalized Ohm's Law is

$$\mathbf{E} + \mathbf{U}_I \times \mathbf{B} = \mathbf{j} \times \mathbf{B}/en - \nabla \cdot \mathbf{P}_e/en + \left(m_e/ne^2\right)\partial \mathbf{j}/\partial t + \eta \mathbf{j} \quad (1)$$

where **E** and **B** are the electric and magnetic fields, $\mathbf{U}_I$ is the velocity of an element of ion fluid, **j** and n are the current and plasma densities, respectively, η is the resistivity associated with ion-electron interactions, and $\nabla \cdot \mathbf{P}_e$ is the divergence of the electron pressure tensor. The first term on the right side of this equation is called the Hall MHD term. *Vasyliunas* [1975] showed that this term becomes important on scale sizes the order of the ion skin depth, c/ω_{pI}, where ω_{pI} is the ion plasma frequency, while the remaining terms on the right side of equation (1) manifest themselves on the 40 times shorter scale, c/ω_{pe}, where ω_{pe} is the electron plasma frequency. Thus, sub-solar magnetopause crossings that do not pass through an electron diffusion region are controlled by the physics of the first term on the right side of equation (1). Because this paper deals with the physics on scale sizes of many ion skin depths, the remaining terms on the right side are neglected in the following discussions.

[3] Two dimensional simulations of Hall MHD physics for reconnecting systems having equal plasma densities and magnetic field strengths on the two sides of the reconnection region showed an out-of-plane quadrupolar magnetic field and in-plane bipolar electric field [*Birn et al.*, 2001]. The out-of-plane quadrupolar magnetic field has positive then negative components across the current sheet on one side of the X-line and negative then positive components on the other side. The in-plane bipolar electric field is normal to the current sheet and points toward the center of the region from either side. These features have been observed in sub-solar magnetopause [*Mozer et al.*, 2002], and tail reconnection events [*Wygant et al.*, 2005] and in the laboratory [*Ren et al.*, 2005]. It is sometimes assumed that the presence of these fields provides necessary and sufficient evidence for reconnection. However, it has been emphasized [*Mozer and Retinò*, 2007] that these field geometries are observed in $\leq$1% of sub-solar reconnection events and it was conjectured that the absence of such fields was a consequence of asymmetric boundary conditions on the two sides of the magnetopause. Theories and simulations of asymmetric reconnection have been published [*Nakamura and Scholer*, 2000; *Borovsky and Hesse*, 2007; *Cassak and Shay*, 2007]. *Pritchett* [2007] has studied the impact of density and magnetic field asymmetries on the quadrupolar B and bipolar E structures with results similar to those reported in this paper.

[4] The absence of the bipolar electric field can be understood through comparing the two measured estimates of the Hall electric field, $\mathbf{E} + \mathbf{U}_I \times \mathbf{B}$ and $\mathbf{j} \times \mathbf{B}/en$. Pioneering comparisons of this type have been reported [*Khotyaintsev et al.*, 2006, and references therein]. In this paper, the first quantitative comparisons are made, based on two sub-solar magnetopause crossings on July 20, 2007 by three of the five THEMIS spacecraft, C, D, and E (the electric field antennas were not yet deployed on the other spacecraft).

2. The Data

[5] The five THEMIS spacecraft were launched on February 17, 2007. On July 20, 2007, the spacecraft were in a string-of-pearls configuration in a 14.7 R_E apogee orbit at locations given in Tables 1 and 2, making two-component electric field (J. Bonnell et al., The electric field experiment on the THEMIS satellites, submitted to *Space Science Reviews*, 2008), plasma (J. P. McFadden et al., The plasma experiments on the THEMIS spacecraft, submitted to *Space Science Reviews*, 2008) and magnetic field (A. U. Auster et al., The THEMIS fluxgate magnetometer, submitted to *Space Science Reviews*, 2008) measurements. Figure 1 presents pairs of panels for each of the three spacecraft that give the spin-period-averaged ion and electron plasma densities in Figures 1a, 1c, and 1e, while Figures 1b, 1d,

[1]Space Sciences Laboratory, University of California, Berkeley, California, USA.
[2]Institute of Geophysics and Extraterrestrial Physics, Technical University of Braunschweig, Braunschweig, Germany.

0094-8276/08/2007GL033033$05.00

Table 1. Spacecraft Locations

	Location
Altitude	11.6 R_E
Magnetic local time	1240
Magnetic latitude, deg	−15

and 1f give three estimates of the spin-period-averaged X-component (sunward) of the electric field as measured by spin plane boom pair 12 (50 m tip-to-tip length), spin plane boom pair 34 (40 m tip-to-tip length) and the ion flow. The plasma density varied from large magnetosheath values to smaller magnetospheric values and then returned to magnetosheath values in Figure 1, which signifies that the magnetopause was crossed a total of six times by the three spacecraft in about six minutes. The excellent agreements between the ion and electron densities and between the three electric field measurements are noted. The ion and boom electric field measurements differ significantly only in the vicinity of the magnetopause crossings. This disagreement is the topic of this paper.

[6] The magnetopause passed over spacecraft C and D nearly simultaneously and after (before) it crossed over spacecraft E on its outbound (inbound) trajectory. Because spacecraft E was mostly earthward of C and D (see Table 2), it is reasonable that the magnetopause motion was mainly in the ±X direction (sunward or tailward), as expected for the sub-solar location of the observations. If this is the case, the ∼100 second difference in the times of the crossings of spacecraft E and the other spacecraft combines with the ∼1400 km X-separation, to give an average magnetopause speed of ∼14 km/sec in the X direction. However, it is not possible to determine an average three-dimensional magnetopause velocity with timing information from only three spacecraft so the magnetopause velocity will be an adjustable parameter in the analyses that follow and it will be found to be this order of magnitude (see Table 3).

[7] Figure 2 presents one minute of data from spacecraft C at each of its magnetopause crossings. Figure 2a gives the ion and electron plasma densities, Figure 2b gives the three components of the magnetic field, Figures 2c, 2d, and 2e give the three components of the electric field as measured by spin plane boom 12, spin plane boom 34, and the ion flow (where the three components of the boom electric fields are obtained with the assumption that the parallel electric field is zero), Figure 2f gives the three components of the total ion flow, Figure 2g gives three estimates of the X-component of the perpendicular flow, and Figure 2h gives the component of energy conversion, $j_Y E_Y$. From Figure 2b (left) it is seen that the reconnecting magnetic field component, B_Z, changed from a small negative value in the magnetosheath to ∼60nT in the magnetosphere and it reversed in the return crossing, as illustrated Figure 2b (right). At both crossings there was an exhaust ion flow,

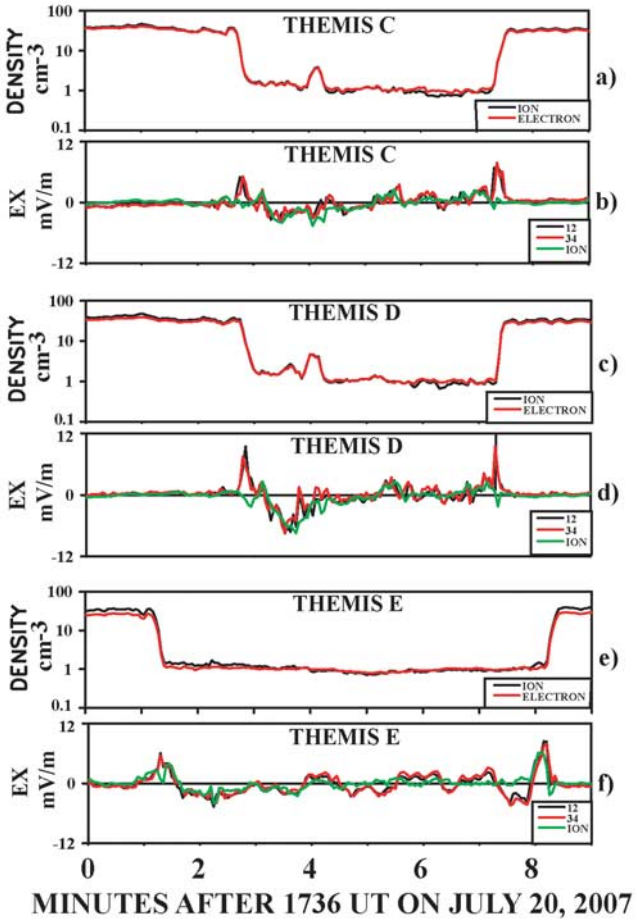

Figure 1. The ion and electron plasma densities and the X-component of the electric field as measured by double probes and the ion flow on three THEMIS spacecraft as the magnetopause passed back-and-forth.

v_Z, whose magnitude in Figure 2f was about equal to the magnetosheath Alfven speed and about half of that computed for asymmetric reconnection with unequal magnetic fields and densities in the two input regions [*Cassak and Shay*, 2007].

[8] The X-directed magnetopause velocities of Table 3 and the typically 15 second duration of the crossings combine to yield magnetopause thicknesses at the locations of the crossings of ∼150 km or about $2-3c/\omega_{pI}$, where the average of the magnetosheath and magnetospheric plasma density has been used in making this estimate.

[9] All data in this paper are translated along the X-axis into the moving magnetopause frame and presented in a joint variance coordinate system [*Mozer and Retinò*, 2007], whose X-axis is in the direction of the maximum variance of E and whose Z-axis is both perpendicular to the X-direction

Table 2. Separations in GSE Coordinates

Direction	C−D	C−E
X, km	425	1410
Y, km	365	−65
Z, km	900	450

Table 3. Boundary Normal Speeds[a]

Spacecraft	Sheath to Sphere	Sphere to Sheath
C	15	−9
D	8	−14
E	25	−20

[a]Speeds are given in km/sec.

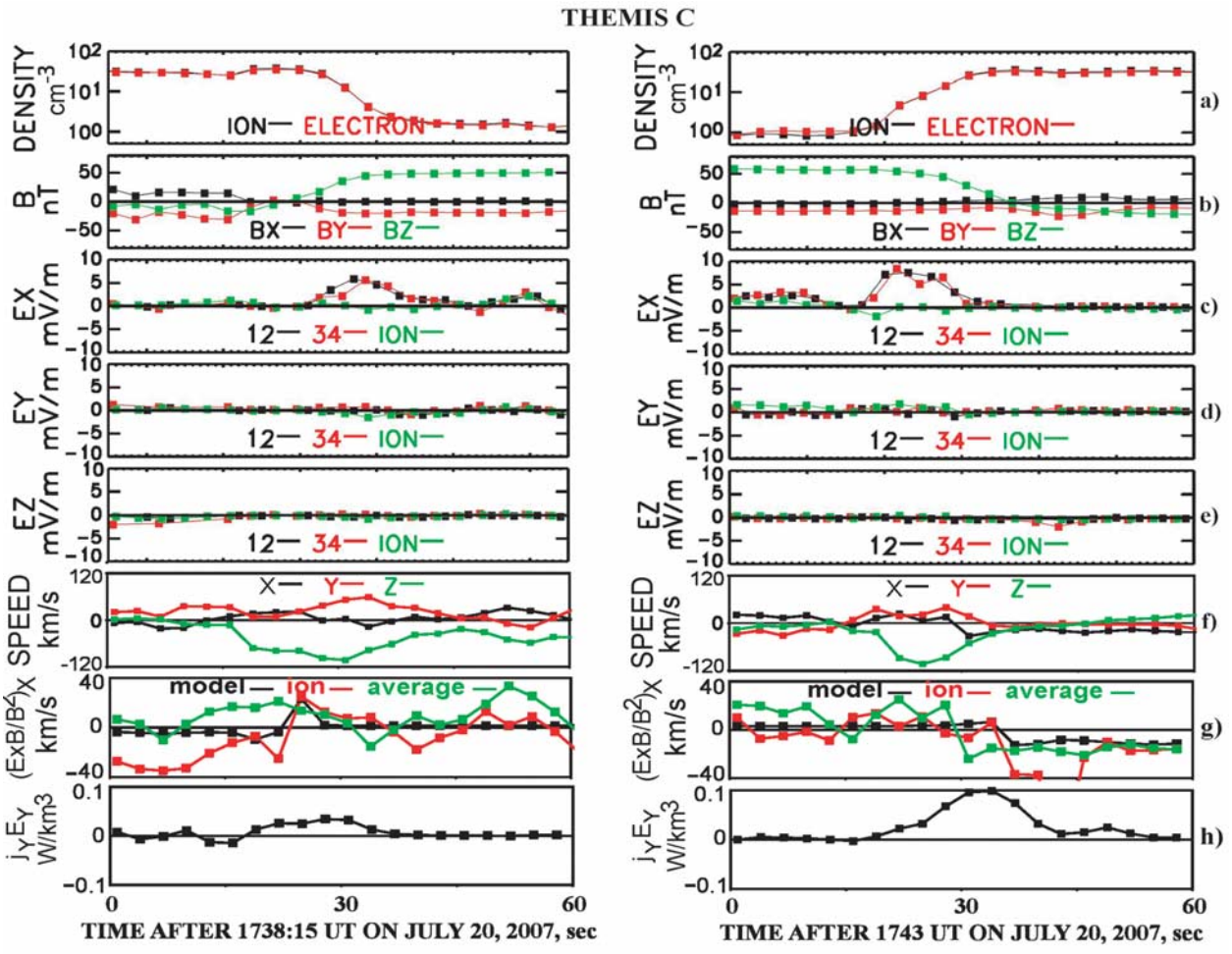

Figure 2. One minute of plasma density, magnetic field, electric field, ion flow, and electromagnetic energy conversion rate data at each of the magnetopause crossings over THEMIS C. The left plots cover the outbound pass of the magnetopause while those on the right describe its return over the spacecraft.

and as nearly as possible along the direction of the maximum variance of the magnetic field as determined from a minimum variance analysis of B. This coordinate system is selected because it allows the normal magnetic field to be a function of X, as it is found to be in asymmetric simulations [*Pritchett*, 2007] and as is not expected from a minimum variance analysis. It is noted that the joint variance X-direction is within a few degrees of the GSE X-direction.

[10] The one-minute-averaged tangential electric field and normal magnetic field are shown in Table 4. The uncertainty in the magnetic field measurement is much smaller than its average value while the uncertainties in the electric field measurement are comparable to the averages. (The uncertainty resulting from the selection of the normal and tangential directions is probably larger and hard to estimate.) For these average values, the reconnection rate (B_X/B_Z or $(E_YB_Z - E_ZB_Y)/B^2V_{ALFVEN}$ at the boundaries) was 2–10%, depending on its definition and the field and density values used [*Mozer and Retinò*, 2007].

[11] Three estimates of the normal component of the perpendicular flow obtained from the measured $(\mathbf{E} \times \mathbf{B}/B^2)_X$, the $(\mathbf{E} \times \mathbf{B}/B^2)_X$ using the above average values, and the perpendicular component of the ion flow, are given in Figure 2g. While the variations of the data probably indicate the uncertainties of the measurements, the three estimates show a tendency for the perpendicular flows to be toward the center of the magnetopause from both sides, confirming that reconnection was occurring because plasma and electromagnetic energy flowed into the magnetopause from both sides. Figure 2h gives j_YE_Y where the average value of the electric field was used and j was obtained as described below. The conversion of electromagnetic energy within the magnetopause is confirmed.

[12] As seen in Figures 2a and 2b, there is a large asymmetry in both the reconnection magnetic field strength and the plasma density on the two sides of the magnetopause, such that the ratio of B_Z/n on the two sides is about 100. It will next be shown that this large asymmetry across

Table 4. One-Minute-Averaged Tangential Electric Field and Normal Magnetic Field

	1738:15–1739:15	1743–1744
B_X, nT	5.36	3.49
E_Y, mV/m	0.18	0.24
E_Z, mV/m	−0.31	−0.18

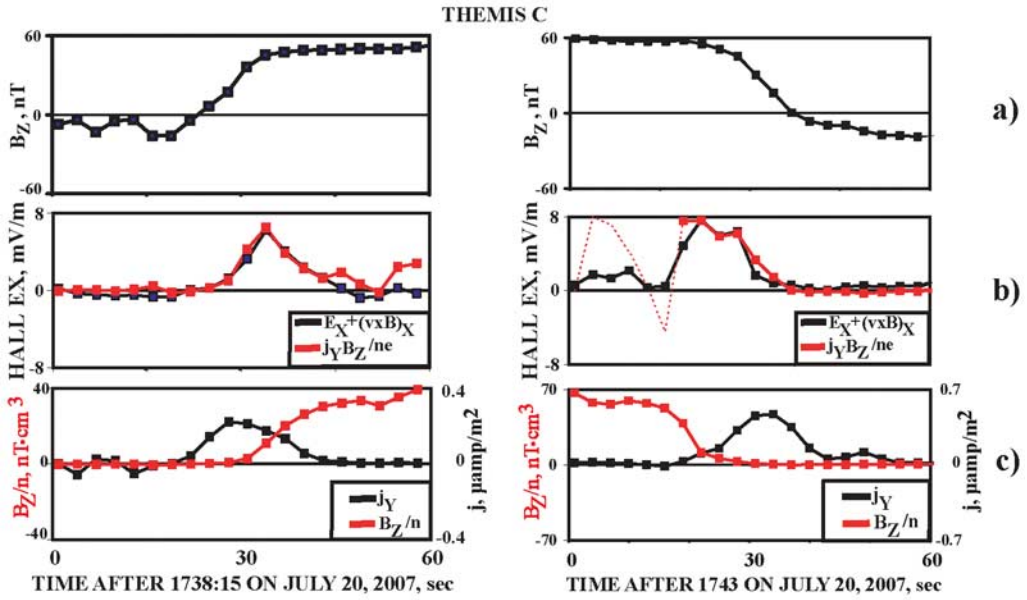

Figure 3. Comparison of $(\mathbf{E} + \mathbf{U_I} \times \mathbf{B})_X$ and $(\mathbf{j} \times \mathbf{B}/en)_X$ for both passages of the magnetopause over THEMIS C. The data illustrate the quantitative agreement between the two terms in the Generalized Ohm's law and illustrate that the explanation of the single peak in the normal electric field is that the ratio of B_Z to the plasma density is too small for a second peak to be important.

the magnetopause determines the properties of the Hall fields.

[13] From Figure 2b, the reconnection magnetic field was about 50 nT and the guide field was about 20 nT at the first crossing and the guide field was smaller at the second crossing. There is little indication of a quadrupolar magnetic field as would be evidenced by a positive then negative excursion (or vice-versa) with time of B_Y across the current sheet. Thus, from the magnetic field point of view, the Hall MHD term in the Generalized Ohm's Law did not manifest itself in the way found in both simulations and observations in which the plasma density and magnetic field in the two asymptotic regions are similar in magnitude.

[14] The boom-measured electric fields and the $-\mathbf{U_I} \times \mathbf{B}$ electric field are in good agreement everywhere in Figure 2 except for the ~15 second current sheet crossings near the center of each plot, where $(-\mathbf{U_I} \times \mathbf{B})_X$ was nearly zero while the X-component of the electric field was 6–8 mV/m in Figure 2c. In this ion diffusion region, the non-zero left side of equation (1) is balanced by the first term on the right side of this equation to produce the Hall MHD electric field. However, contrary to expectations from symmetric simulations, the Hall MHD electric field of Figure 2c and of Figure 3b is unipolar and not bipolar.

[15] In Figure 3b, the X-component of the left side of equation (1) is compared with the X-component of the first term on the right side of equation (1). The dashed curve in Figure 3b of the second crossing is uncertain because uncertainties in the estimate of j_Y are multiplied by a factor of 100 to produce the Hall term in this region. The reconnection magnetic field is given in Figure 3a to provide a reference as to where the Hall MHD term was important during the crossing. $(\mathbf{E} + \mathbf{U_I} \times \mathbf{B})_X$ was obtained from direct plasma and field measurements, while the current density, j_Y, in the first term on the right, $(\mathbf{j} \times \mathbf{B}/en)_X = j_YB_Z/en$ was obtained from measurements and Amperes Law as

$$j_Y = (\Delta B_Z/\Delta t)/\mu_0 v \quad (2)$$

where Δt was selected to be 6 seconds in order to have a time interval that was long enough to minimize statistical fluctuations while being shorter than the crossing time, and v is the speed of the magnetopause across the spacecraft in the X-direction. The only adjustable parameter in this analysis is this constant magnetopause speed, v, which was set to +15 and −9 km/sec for the two crossings of Figure 3. Table 3 gives the speeds of the magnetopause at the six crossings observed by the three spacecraft.

[16] In Figure 3b, the Hall MHD electric field is significant only on the magnetospheric side of the magnetopause. The explanation of the missing peak on the magnetosheath side of the magnetopause is given in Figure 3c in which the product of a constant and the two plots in Figure 3c is the Hall electric field. Because B_Z/n is very small on the magnetosheath side of the magnetopause, the Hall electric field in this region is also small.

[17] For a bipolar electric field in the X-direction, the ions entering the magnetopause from either side are first accelerated through this electric potential and then decelerated by the identical potential on the other side of the magnetopause. Thus, they bounce back and forth across the magnetopause while moving in the Z-direction to leave the active region with the Alfven speed [*Wygant et al.*, 2005]. In the absence of the X-directed electric field at the magnetosheath side of the magnetopause, the single particle ion trajectories are different. Thus, in this case, the Hall MHD term is important but in a way that is different from that

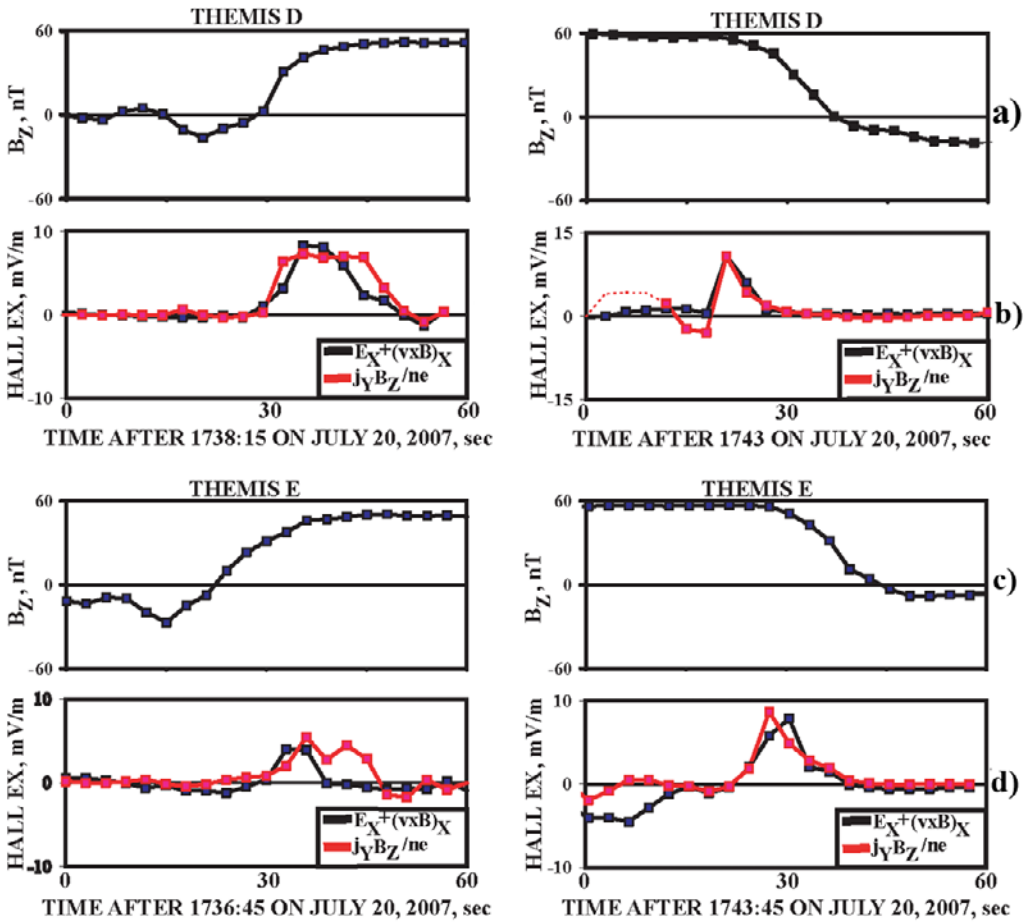

Figure 4. Comparison of $(\mathbf{E} + \mathbf{U}_I \times \mathbf{B})_X$ and $(\mathbf{j} \times \mathbf{B}/en)_X$ for the pair of magnetopause crossings over THEMIS D and THEMIS E. The data illustrate the quantitative agreement between the two terms in the Generalized Ohm's law.

found in simulations having B_Z and the plasma density similar in magnitude on the two sides.

[18] The effect on particles of this difference of field geometries between symmetric reconnection and the THEMIS data of July 20, 2007 can be explored by consideration of Figure 2h in which $j_Y E_Y$ is plotted as a function of time by using the tangential electric field averages given above. The electromagnetic energy conversion associated with this current is $0.04-0.1$ W/km^3. Dividing this energy conversion rate by a typical plasma density of 10 particles/cm^3 yields an energy conversion rate of $\sim$20–50 eV/particle-sec. Because 100 km/sec protons in the outflow have an energy of $\sim$50 eV, such protons must have stayed in the energy conversion region for the order of a second. The outflowing ions came predominately from the magnetosheath because the plasma density in the outflow is more than an order-of-magnitude larger than that in the magnetosphere. The X-directed Hall electric field that these ions experience is repulsive so it cannot directly explain the ion energization. In fact the Hall electric potential of $\sim$1 kV is sufficient to stop the typical 0.5 keV magnetosheath protons. Thus, the asymmetric reconnection problem must involve particle trajectories and mechanisms different from those associated with symmetric reconnection.

[19] Figure 4 presents data for the two magnetopause crossings encountered by each of spacecraft D and E. In each case, the conclusion is the same as that for the spacecraft C crossings. Namely, there is a single peak in the Hall electric field because B_Z/n is sufficiently small in the magnetosheath side of the crossing that the Hall term is negligible there. From Table 3 it is seen that all outbound magnetopause traversals (from the magnetosheath to the magnetosphere as seen by the spacecraft) had positive speeds while the inbound crossings had negative speeds. This fact adds confidence to the single parameter fit that determines the Hall electric field for each of the crossings.

[20] **Acknowledgments.** The achievement of building five spacecraft on time and on a limited budget and having them perform flawlessly is due to the diligent efforts of many people whom we thank profusely. This work was supported by NASA grant NNG05GC72G and contract NAS5-02099-07/09, and by grant 50QP0402 from the Deutsches Zentrum für Luft- und Raumfahrt and the German Ministerium für Wirtschaft und Technologie.

References

Birn, J., et al. (2001), Geospace environmental modeling (GEM) magnetic reconnection challenge, *J. Geophys. Res.*, *106*, 3715.

Borovsky, J. E., and M. Hesse (2007), The reconnection of magnetic fields between plasmas with different densities: Scaling relations, *Phys. Plasmas*, *14*, 102309.

Cassak, P. A., and M. A. Shay (2007), Scaling of asymmetric magnetic reconnection: General theory and collisional simulations, *Phys. Plasmas*, *14*, 102114.

Khotyaintsev, Y. V., et al. (2006), Formation of inner structure of a reconnection separatrix region, *Phys. Rev. Lett.*, *97*, 205003.

Mozer, F. S., and A. Retinò (2007), Quantitative estimates of magnetic field reconnection properties from electric and magnetic field measurements, *J. Geophys. Res.*, *112*, A10206, doi:10.1029/2007JA012406.

Mozer, F. S., S. D. Bale, and T. D. Phan (2002), Evidence of diffusion regions at a sub-solar magnetopause crossing, *Phys. Rev. Lett.*, *89*, 015002, doi:10.1103/PhysRevLett.89.015002.

Nakamura, M., and M. Scholer (2000), Structure of the magnetopause reconnection layer and of flux transfer events: Ion kinetic effects, *J. Geophys. Res.*, *105*, 23,179.

Pritchett, P. L. (2007), Collisionless magnetic reconnection in an asymmetric current sheet: implications for magnetopause reconnection, *Eos Trans. AGU*, *88*(52), Fall Meet. Suppl., Abstract SH43A-07.

Ren, Y., et al. (2005), Experimental verification of the Hall effect during magnetic reconnection in a laboratory plasma, *Phys. Rev. Lett.*, *95*, 055003.

Vasyliunas, V. M. (1975), Theoretical models of magnetic field line merging, *Rev. Geophys.*, *13*, 303.

Wygant, J. R., et al. (2005), Cluster observations of an intense normal component of the electric field at a thin reconnecting current sheet in the tail and its role in the shock-like acceleration of the ion fluid into the separatrix region, *J. Geophys. Res.*, *110*, A09206, doi:10.1029/2004JA010708.

V. Angelopoulos, J. Bonnell, J. P. McFadden, and S. Mozer, Space Sciences Laboratory, University of California, Berkeley, CA 94720, USA. (fmozer@aol.com)

K. H. Glassmeier, Institute of Geophysics and Extraterrestrial Physics, Technical University of Braunschweig, D-38106 Braunschweig, Germany.